ON THE MECHANICAL PROPERTIES OF AN H-C RUBBER

Wolfgang G. Knauss
Firestone Flight Sciences Laboratory
Graduate Aeronautical Laboratories
California Institute of Technology

1.1.3
1.4
1.3.2

ABSTRACT

The material properties of H-C binder including dynamic shear compliance, relaxation modulus, creep compliance, ultimate stress and ultimate strain are reported. Further useful information in the form of Modified Power Law and Prony Series curve fits are included as well as a master curve of reduced stress vs. strain.

All tests are performed using standard procedures; however some inconsistancy in material properties has been found. It was further determined that the time-temperature shift principle is not directly applicable in its simplest form; however, upon postulating two molecular mechanisms responsible for gross deformations it is found that each one can be associated with a different characteristic glass transition temperature such that, e.g. the dynamic compliance J(w) is the sum of two compliances J_α and J_γ

$$J(w, t) = J_\alpha\ (w,\ T^\alpha{}_{glass}) + J_\gamma(w,\ T^\gamma{}_{glass})$$

which individually follow the time temperature superposition principle.

INTRODUCTION

The work described in this paper was initially intended to cover routine determination of mechanical properties of an H-C rubber used in crack propagation studies by the author. The fact that there was no intent on studying the material properties for any particularly interesting effects will be apparent through the absence of any special test procedures other than those usually employed in engineering practice. Since the determination of dynamic shear compliance in a Fitzgerald and Ferry twin transducer (Ref. 2) is usually considered to be a rather accurate method, it was hoped that the dynamic data would indicate the accuracy with which uniaxial tensile data could be used to obtain the relaxation modulus. This aim has been partially satisfied inasmuch as it has been found that any possible deviation from the conventional time-temperature superposition principle could not have been deduced from test data because of the lack of data accuracy. On the other hand a large discrepancy between the rubbery modulus as determined in a direct tensile creep test and as calculated from dynamic shear compliance data questions the validity of the dynamic tests*. Barring any gross errors in data reduction or equipment failure the present work points out that some, apparently hitherto unknown, problems exist in mechanical properties determination and that double experimentation of the type described herein may not only prove useful but may be mandatory for certain applications.

* A repetition of the dynamic tests will probably be conducted after the equipment has been overhauled.

The material tested is a carboxy terminated polymer, commercially produced as H-C rubber, but prepared for experimental purposes. No detailed information on the molecular structure is known so that the relation of the results described here to the physio-chemical structure of the rubber must, for the present at least, remain a matter of conjecture and perhaps a subject of further study.

DYNAMIC SHEAR COMPLIANCE

The dynamic shear compliance was measured on a Fitzgerald and Ferry twin transducer; Data was obtained by testing at six different frequencies, covering approximately 1 decade of frequency, while holding the temperature constant at sixteen different temperatures in the range -60° to 21° C. In order to obtain a check on thermal and mechanical degradation of the test samples the temperature range was traversed from warm to cold temperatures and reverse: No significant difference between the two sets of data was observed.The compliance values thus obtained were reduced to a standard temperature of T_o=226°K by the usual density-temperature ratio, i.e.

$$J'_p = J' \frac{\rho(T)\cdot T}{\rho(T_o)\cdot T_o} \qquad J''_p = \frac{\rho(T)\cdot T}{\rho(T_o)\cdot T_o} \quad * \qquad (1)$$

where J' and J'' are the measured real and imaginary parts of the complex compliance, respectively. The reduced compliances J'_p and J''_p are shown as a function of temperature and frequency in figures 1 and 2.

From figure 2 it is immediately obvious that the time-temperature shift principle does not apply directly, for the value of the relative minimum in the J''_p vs. temperature areas is a function of frequency. Indeed an attempt at superposing J'_p and J''_p by the same shift factor leads to an inconsistancy for temperatures above -35° C which cannot be explained through data inaccuracy. From figure 1 it appears that below -30°C the real compliance behaves in an expected manner and that at higher temperatures an additional compliance enters the measurements. With the possibility of two simultaneously operative deformation mechanisms, assume a reduced compliance J'_p as shown in figure 1 and further assume that the time-temperature shift phenomenon as governed by the WLF equation is applicable at temperatures above -35°C as it is below -35°C**; This is shown in figure 3 with the appropriate temperature-shift factor relation presented in figure 5A. Subtract this compliance J_p ' from the measured values to obtain the difference J_{pv}' ; this is presented as a function of temperature and frequency in figure 4. Due to the numerical conversion from logarithmic values to actual values and subtraction the accuracy has somewhat suffered, but does not at all appear disturbing. Superposition of the data in figure 4 results in the temperature-shift

* The density was determined to better than 1/4 % accuracy to be $\rho(\theta) = \{0.9205 - 6.19 * 10^{-4}(\theta - 22.5)\}$ gm/cm^3 , $[\theta]$ = °C.

** The author is here indebted to Dr. Landel for calling his attention to the so-called β mechanism reported in the literature (Ref. 3).

factor relation shown in figure 5B and the "master" plot, figure 6. It is noteworthy that inspite of the uncertainty in assuming a part of the α-compliance the separation of the experimental data into two compliances

$$J'_p = J'_{p\alpha} + J'_{p\gamma} \tag{2}$$

has resulted in time-temperature superposable curves which separately follow the WLF superposition scheme remarkably well. It is further of interest to note that the "glass transition temperatures" for the two separated mechanisms are, according to the WLF scheme, at -90°C and -63°C; A careful dilatometric study* determined this temperature as -87°C and no second transition temperature was found near -63°C.

The critical test for this type of data decomposition would be the calculation of the imaginary part of the compliance from the decomposed real parts. Since shorter, approximate methods are not deemed sufficiently accurate to provide a test and since exact conversion is time consuming due to the numerical nature of the calculations** this test has not yet been performed.

DETERMINATION OF RELAXATION MODULUS FROM DYNAMIC SHEAR COMPLIANCE

If the relaxation shear modulus is expressed as

$$\mu_{rel}(t) = \mu_{eq} + \sum_{n=1}^{N} \mu_n e^{-t/\tau_n} \tag{3}$$

where μ_{eq} is the rubbery shear modulus and equal to $1/J'_p(w=0)$, τ_n are the relaxation times and N is sufficiently large, then the shear stress $\tau(t)$ in a test with oscillatory strain input, $\varepsilon(t) = \varepsilon_o e^{i\omega t}$, can be found with Duhamel's Integral to be

$$\tau(t) = \varepsilon_o \mu_{eq} e^{i\omega t} + \varepsilon_o \int_o^t (\mu_{rel}(\theta) - \mu_{eq}) i\omega e^{i\omega(t-\theta)} d\theta$$

or

$$\frac{\tau(t)}{\varepsilon_o} - \mu_{eq} e^{i\omega t} = i\omega e^{i\omega t} \sum_{n=1}^{N} \mu_n \int_o^t e^{-\left(\frac{1}{\tau_n} + i\omega\right)\theta} d\theta \tag{4}$$

The complex shear modulus is then given by

$$\mu^*(\omega) = \lim_{t\to\infty} \frac{\tau(t)}{\varepsilon_o e^{i\omega t}} = \mu_{eq} + \sum \frac{\mu_n i\omega\tau_n}{1 + i\omega\tau_n} \tag{5}$$

As $\mu^*(\omega) = 1/(J'_p(\omega) + iJ''_p(\omega))$ the moduli μ_n can be determined in a curve fit; this has been done for N = 18. If one assumes that Poisson's ratio is a constant and equal to 1/2 then the tensile relaxation modulus $E_{rel}(t)$ is given by

$$E_{rel}(t) = 3\left\{\mu_{eq} + \sum_{n=1}^{17} \mu_n e^{-t/\tau_n}\right\}; \tag{6}$$

this relation is shown in figure 10 as the dashed curve. Because of the limited temperature range over which the material could be tested the

* The author is again indebted to Dr. Landel for having this study performed.
** See, e.g. reference (4).

glassy modulus was estimated from related data as described in the following section and the rubbery modulus calculated with the help of extrapolation in figure 6. For later reference it is important to note, that the extrapolation is not the reason for the low modulus, nor that the equilibrium compliance or modulus is affected by the conversion of equations 4, 5 and 6. Indeed a quick calculation with the real part of the compliance, figure 1, will show that the equilibrium modulus must be smaller than 45 psi.

MEASUREMENT OF THE RELAXATION MODULUS

Only a limited amount of direct relaxation data has been obtained. Whereas the deviation from the relaxation modulus as determined in the following is not great there is need to also perform more extensive relaxation tests and to compare the results with those obtained as described below.

It has been shown (Ref. 5) that the relaxation modulus can be determined in a constant strain rate tensile test from the relation

$$E_{rel}(t) = \left.\frac{d\sigma}{d\epsilon}\right|_{\epsilon=Rt} \tag{7}$$

where R is the strain rate; in other words the relaxation modulus for a linearly viscoelastic material at time t is the slope of the stress strain curve in a constant strain rate test evaluated at the strain $\epsilon=Rt$. Writing the slope alternately as

$$\frac{d\sigma}{d\epsilon} = \frac{\sigma}{\epsilon}\frac{d\log\sigma}{d\log\epsilon} = \frac{\sigma}{\epsilon}\frac{d\log\sigma/R}{d\log\epsilon/R} \tag{8}$$

it is seen that a plot of σ/R vs. ϵ/R on log-log paper will provide the time dependent correction factor in the form of the log-log slope to the usual modulus definition σ/ϵ ; if tests at different temperatures are run, a plot as shown in figure 7 is obtained. The correction factor $(1+\epsilon)$ in figure 7 accounts for the small non-linearity of the material as strains of up to 10% were employed for this plot, and the ratio T_o/T is the standard temperature reduction employed in viscoelastic data analysis (Ref. 6). If one writes the temperature reduced strain rate Ra_T in place of the strain rate, equation (8) becomes

$$\frac{d\sigma}{d\epsilon} = \frac{(1+\epsilon)\frac{T}{T_o}\sigma/Ra_T}{\epsilon/Ra_T}\,\frac{d\log(1+\epsilon)\frac{T}{T_o}\sigma/Ra_T}{d\log\epsilon/Ra_T} \tag{9}$$

and it is seen that the individual curves in figure 7 can be used to compose one master curve if they are shifted equal amounts along the $\log\epsilon/R$ and $\log[\sigma(1+\epsilon)T_o/TR]$ axis, i.e. along a line of unit slope in figure 7, provided, of course, that the time-temperature shift scheme is admissible.

Without any reference to the work reported in the previous sections such a shift was effected and the resulting master stress-strain wave is shown in figure 8. The corresponding temperature-shift factor is given in figure 9. Two observations are of interest: Part of the points fall on the curve predicted by the WLF relation, if the glass transition temperature is taken to be -80°C which is the value reported by the supplier. Second, those

points which do not fall on the same curve are derived from the curves in figure 7 which have almost unit slope and are not amenable to accurate shifting when the scatter in data is considered. However it is noteworthy that quite a similar deviation from the WLF equation is observed if one attempts to shift the real part of the dynamic compliance under neglect of the imaginary part. It appears therefore that a more carefully conducted uniaxial test could also be used to observe any abnormalities in a material.

The relaxation modulus obtained from the master curve is shown in figure 10 and figure 11 shows the corresponding line relaxation spectrum of a 17 element model. The glassy modulus has been estimated from stress-strain curve slopes at low temperatures and high strain rates where the material appeared to behave elastically. For reference the modified power law approximation (4) to the relaxation modulus is also shown.

Much more disturbing than the breakdown in the time-temperature superposition principle is the fact that the rubbery modulus evinces such a high discrepancy when obtained by different methods; as another independent check it was measured by suspending 100 gms. from a rubber strip with 1/16 in.^{2} cross-section, carrying benchmarks six inches apart in the unstrained condition. The strain after 1/2 hour was used to measure the rubbery modulus as 123 psi, which value would also be commensurate with that calculated from the dynamic compliance of the α-compliance with disregard of the γ-compliance. Note from figure 9 that the 1/2 hour time interval is sufficient to permit the calculation of the rubbery modulus in this manner.

CREEP COMPLIANCE

Although the creep compliance can be calculated from the dynamic compliance data of, e.g. figure 1, it is instructive to determine the compliance from the relaxation modulus. Writing the relaxation modulus $E_{rel}(t)$ as

$$E_{rel}(t) = E_{eq} + \sum_{n=1}^{17} E_n e^{-t/\tau_n} \tag{10}$$

where, in terms of equation (6), $E_{eq} = 3\mu_{eq}$ and $E_n = 3\mu_n$ writing the creep compliance in a similar expression as

$$D_{crp}(t) = D_{eq} - \sum_{n=1}^{17} D_n e^{-t/\tau_n} \tag{11}$$

it is only necessary to determine the D_n from the relaxation modulus (10). This is accomplished most easily by Laplace transforming equations (10) and (11), and noting that the following relation holds between the transforms $\overline{D}_{cr}(p)$ and $\overline{E}_{rel}(p)$ (Ref. 4)

$$D_{crp}(p) \cdot E_{rel}(p) = \frac{1}{p^2} \tag{12}$$

In terms of the series expressions (10) and (11), the relation (12) can be written as

$$D_{eq} - \sum_{n=1}^{17} \frac{D_n p\tau_n}{1 + p\tau_n} = \frac{1}{E_{eq} + \sum_{n=1}^{17} \frac{E_n p\tau_n}{1 + p\tau_n}} \qquad (13)$$

By using the collocation method proposed by Schapery (Ref. 7) and collocating the left hand side to the right hand side at 17 values of $P_k = 1/\tau_k$ equation (13) reduces to the form of a matrix equation

$$[A_{kn}][D_n] = [\phi(P_k)] \qquad n, k = 1, 2, \cdots, 17. \qquad (14)$$

where

$$A_{kn} = \frac{P_k \tau_n}{1 + P_k \tau_n} \quad ; \quad \phi(P_k) = \frac{1}{E_{eq}} - \frac{1}{E_{eq} + \sum_{n=1}^{17} \frac{E_n P_k \tau_n}{1 + P_k \tau_n}}$$

Solution of the matrix equation (14) (simultaneous solution of the 17 equations for the 17 unknowns D_n) determines therefore the creep compliance (11).

While this determination of the creep compliance is exact within the limitations of the model representation of viscoelastic materials, it is interesting to compare the result of the ad hoc relation of the creep compliance to the relaxation modulus

$$D_{crp}(t) \doteq \frac{1}{E_{rel}(t)} \qquad (15)$$

The result of the more exact calculation is compared with that of equation (15) in figure 12*. A simple approximation analogous to the modified power law representation of the relaxation modulus is also shown in the same figure.

ULTIMATE PROPERTIES

The tensile specimens and test procedure employed were similar to those employed by Smith (Ref. 9): circular rings of approximately one inch diameter and 1/8 x 1/8 inch cross section were pulled in an Instron at constant cross-head speeds between 1/4 inch diameter steel hooks. The dimensions of the rings were obtained after rupture by measuring the cross-section at the break section on a comparator and the average length of the rings by unrolling them without stretching. In order to obtain an estimate of the accuracy of measurements the weight of the specimen was plotted against the calculated volume. The deviation was at most 5% and usually not more than 3%. The density was determined to be 0.91 gm/cm^3 which compares well with the value of 0.92 gm/cm^3 at room temperature given in the footnote on page 2.

* The relatively good agreement for the two methods was anticipated by Schapery (Ref. 8) on analytical grounds. This is a result of the relatively small slope of the log E_{rel} vs. log t curve in the transition region (Ref. 4).

The ultimate stress and strain are shown as functions of the temperature reduced strain rate in figure 13. At low temperatures yielding of some samples was observed accompanied by a local reduction in area. The ensuing yield flow contributed much to increasing the ultimate strain and the area reduction increased the true stress. However no correction has been made for this effect, and since the yield stress was never markedly different from the rupture stress the rupture stress based on the undeformed cross-section has been plotted consistently.

Similarly the flow of material around the suspension hooks was impaired at low temperatures. A rough estimate of the effective increase in ultimate strain has been shown as vertical lines in the composite curve.

Superposition of the test data to obtain the composite curves of figure 13 was performed on the stress and strain data simultaneously, resulting in a single temperature shift relation which follows the WLF relation very well except again at temperatures above 0°C, when the experimental points fall below that relation like in figure 9, although the deviation is not as marked. The glass temperature deduced from the WLF equation for the ultimate properties data was found to be -63°C, which is precisely the glass temperature found for the γ-mechanism in the reduction of the shear compliance data.

THE EFFECT OF FILLER

Figure 10 shows also the relaxation modulus for an H-C solid rocket propellant and figure 14 a comparison of the ultimate properties for the filled and unfilled H-C rubber. Although the precise composition for neither the binder nor the propellant are available for reasons of proprietory and security regulations, it suffices to state that the chemical functionality of the curing agent, the pure binder being the result of a higher functionality of the curing agent than the binder in the propellant; this would account for the relatively small difference in the elastic moduli of the binder and the propellant, since the rubbery modulus increases with the amount of cross-linkage which is proportional to the functionality of the curing agent. One would expect that the total relaxation modulus would be effected in a similar fashion, and that for a rigorous comparison the relaxation modulus curve in figure 10 would have to be shifted downward by an unknown amount. With such adjustments in mind it is interesting to make some observations on the effect of filler in the material.

We note that all curves for the propellant are to the right of the binder curves. Physically this may be interpreted as a slow down effect of the filler on gross deformation rate processes in the material. Since the binder should relax at the same rate whether unfilled or as part of the filled composite it would follow that the extra retardation in the rate processes leading to relaxation is due to the interaction of the filler and binder and the interference of the filler with itself (for high filler content). However notice that where the times of relaxation differ by approximately six to eight decades for the filled and unfilled material the failure times ($\sim$ inverse of strain rate) differ by merely two decades as evident in figure 14. It appears therefore that the filler has a more pronounced effect in properties which depend on the small motion of filler particles where the resistance of the filler granules to motion is important. On the other hand

where strength properties rather than motions are concerned the filler does not affect the internal rate processes as severely. However, in the latter case the absolute values of the properties are affected because strength properties depend on the bonding strength between filler and binder, and once dewetting has occurred on the strength of the binder alone. At that instance the dewetted filler acts effectively as a net area reducer so that the binder breaks at the same true stress but the whole sample at a lower engineering stress. A related phenomenon is the reduction in maximum ultimate strain for the simple reason that the relatively rigid filler does not contribute significantly to the strain; for a rubber containing 70 % rigid filler one should expect approximately a 70% reduction in ultimate strain which appears reasonable in view of figure 14. Furthermore it appears from the relaxation modulus in figure 10 that at strain rates higher than 10^9 in/in/min the propellant behaves glass like and hence the rupture strain should be correspondingly small: This is again borne out by figure 14. We are thus able to limit the ultimate tensile strain from the ultimate properties of the binder and knowledge of the relaxation modulus of the propellant.

Although these considerations are mostly qualitative; it appears feasible to employ a detailed analysis of the processes occurring in filled rubbers and to arrive at usable quantitative results.

CONCLUSION

In summary we find two phenomena not commonly reported with the mechanical properties of polymers: the possible existence of two molecular deformation mechanisms with different temperature dependence and a value of the equilibrium modulus which depends on the type of test used. The possibility that the modulus discrepancy is due to faulty test equipment (poor temperature control) is contradicted by the apparently nice reduction achieved with the two polymer-molecular mechanisms, through standard means and by the repeated appearance of the characteristic glass transition temperature for one of the molecular mechanisms and the failure data, $T_g = -63^oC$.

One is obviously tempted to further hypothesize on a possible relation of the postulated γ-mechanism with the failure behavior as the γ-compliance is not due to thermal or mechanical degradation as has been checked by duplication of the dynamic tests. One is therefore left with the possibility of a rubber network which consists of the basic cross-linked network and more or less loose chain ends or chain aglomerates which uncoil only under the to-and-fro motion of a dynamic test but not under constant load or strain such as in a creep test; if the uncoiling or uncoupling of such a rate-structure is a prerequisite to total rupture, the coincidence of the glass transition temperature for the two processes would be at least partially explained, and it would further explain the discrepancy observed in the equilibrium moduli. The concept of changes in entanglement coupling at higher temperatures and lower frequency would appear to be a useful guide in designing an experiment to further illucidate this speculation. For this purpose it would be necessary to conduct dynamic tests at truly low frequencies instead of relying on the time-temperature shift principle.

ACKNOWLEDGMENTS

This investigation was made possible in part by the National Aeronautics and Space Administration Research Grant No. NsG 172-60, GALCIT 120. Thanks are due to Mr. John Clauser and Mr. Jon Kelly of the California Institute of Technology for conducting the dynamic shear and constant strain rate tests and to Mr. Bill Moser of the Jet Propulsion Laboratory for his supervision of the dynamic compliance measurements. Special gratitude is due to Dr. Robert Landel of the Jet Propulsion Laboratory for making his test equipment so readily available, and for his personal interest and help in data reduction. It is hoped that further analysis of these material properties will be carried out with his cooperation. The cooperation of Mr. G. H. Lindsey during the revision is gratefully acknowledged.

The material was obtained from the Thiokol Chemical Corporation, Huntsville, Alabama, through the courtesy of Drs. T. Neely and R. B. Kruse. The data on filled H-C rubber has been taken from reference 1.

REFERENCES

1. Kruse, R. B.: "The Role of Broad-Spectrum Mechanical Responses Studies in Propellant Evaluation." 20th Meeting Bulletin of the JANAF Panel on Physical Properties of Solid Propellants, Vol. 1, November 1961. Riverside, California, p. 395. (SPIA/PP14u).

2. Fitzgerald, E. R.; Ferry, J. D.: Journal of Colloid Science, Vol. 1. p. 1, 1953.

   Fitzgerald, E. R.: Phys. Review, Vol. 108, p. 690, 1957.

3. Ferry, J. D.: Viscoelastic Properties of Polymers, John Wiley and Sons, New York, 1961, pp. 235.

4. Williams, M. L.; Blatz, P. J.; Schapery, R. A.: Fundamental Studies Relating to Systems Analysis of Solid Propellants. GALCIT SM 61-5, California Institute of Technology, Pasadena, California, p. 32. ASTIA Report No. AD 256-905.

5. Ibid, p. 29.

6. Ferry, J. D.: loc cit: p. 205.

7. Schapery, R. A.: Irreversible Thermodynamics and Variational Principles with Applications to Viscoelasticity, Dissertation, California Institute of Technology, June 1962. Published as ARL 62-418, August 1962, USAF, Dayton, Ohio.

8. Schapery, R. A.: Personal communication, January 1963.

9. Smith, T. L.: "Dependence of Ultimate Properties of a GR-S Rubber on Strain Rate and Temperature. Journal of Polymer Science, Vol. 32, p. 99, 1958.

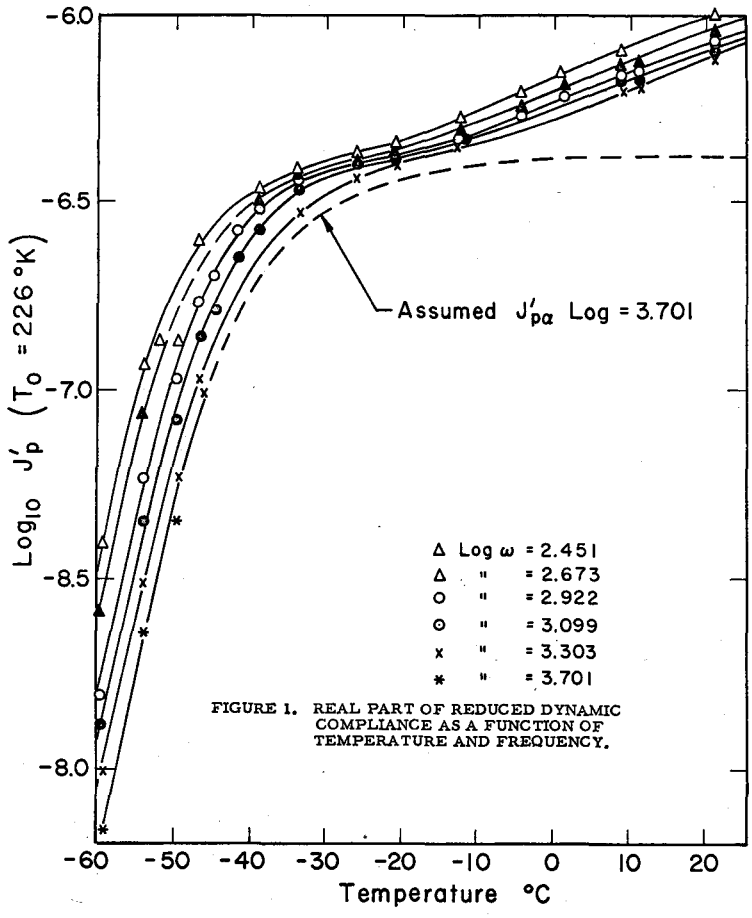

FIGURE 1. REAL PART OF REDUCED DYNAMIC COMPLIANCE AS A FUNCTION OF TEMPERATURE AND FREQUENCY.

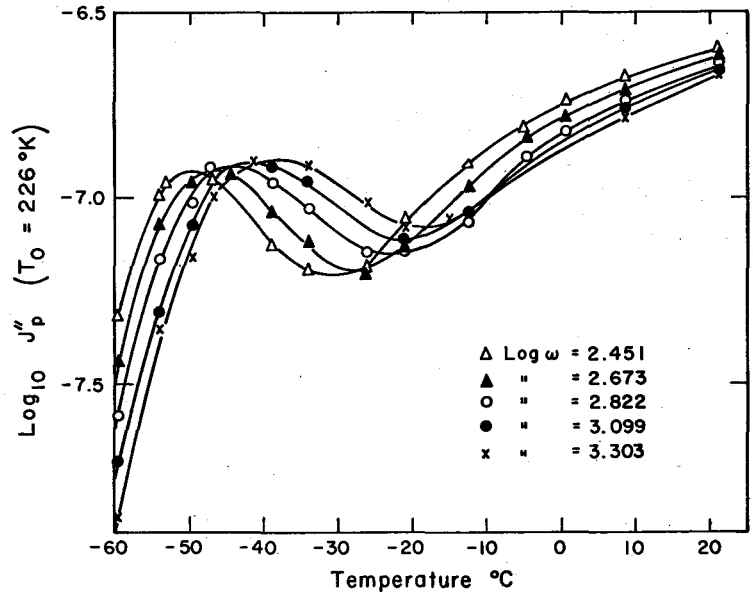

FIGURE 2. IMAGINARY PART OF REDUCED DYNAMIC COMPLIANCE AS A FUNCTION OF TEMPERATURE AND FREQUENCY.

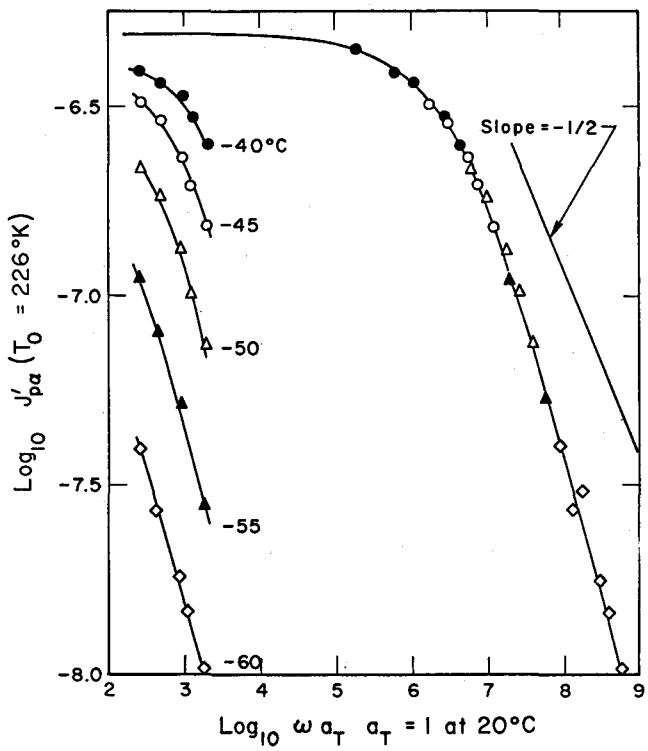

FIGURE 3. REAL PART OF ALPHA DYNAMIC COMPLIANCE (COMPOSITE).

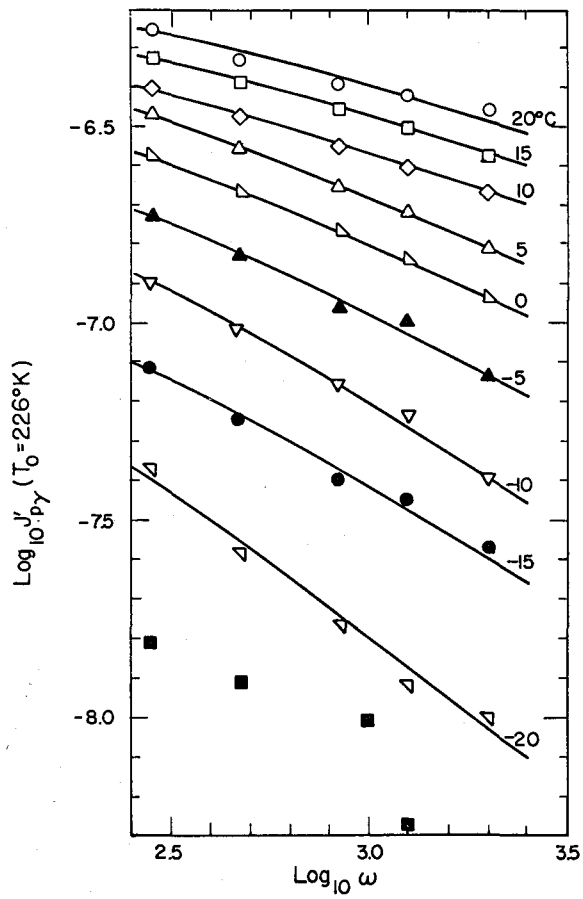

FIGURE 4. REAL PART OF GAMMA DYNAMIC COMPLIANCE.

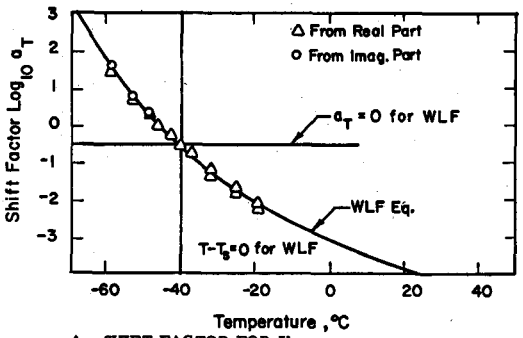

A. SHIFT FACTOR FOR $J'_{p\alpha}$

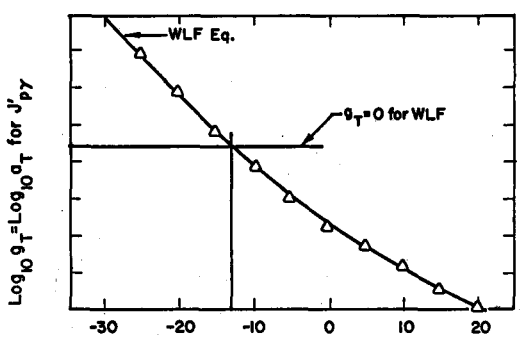

B. SHIFT FACTOR FOR $J'_{p\gamma}$

FIGURE 5. SHIFT FACTORS.

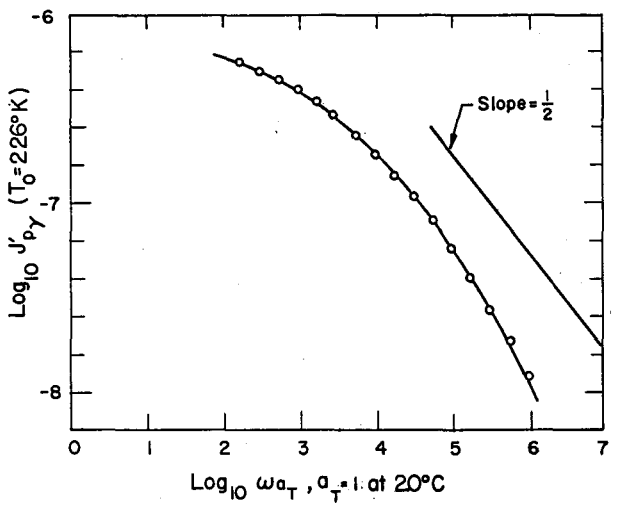

FIGURE 6. REAL PART OF GAMMA DYNAMIC COMPLIANCE (COMPOSITE REPRESENTATION).

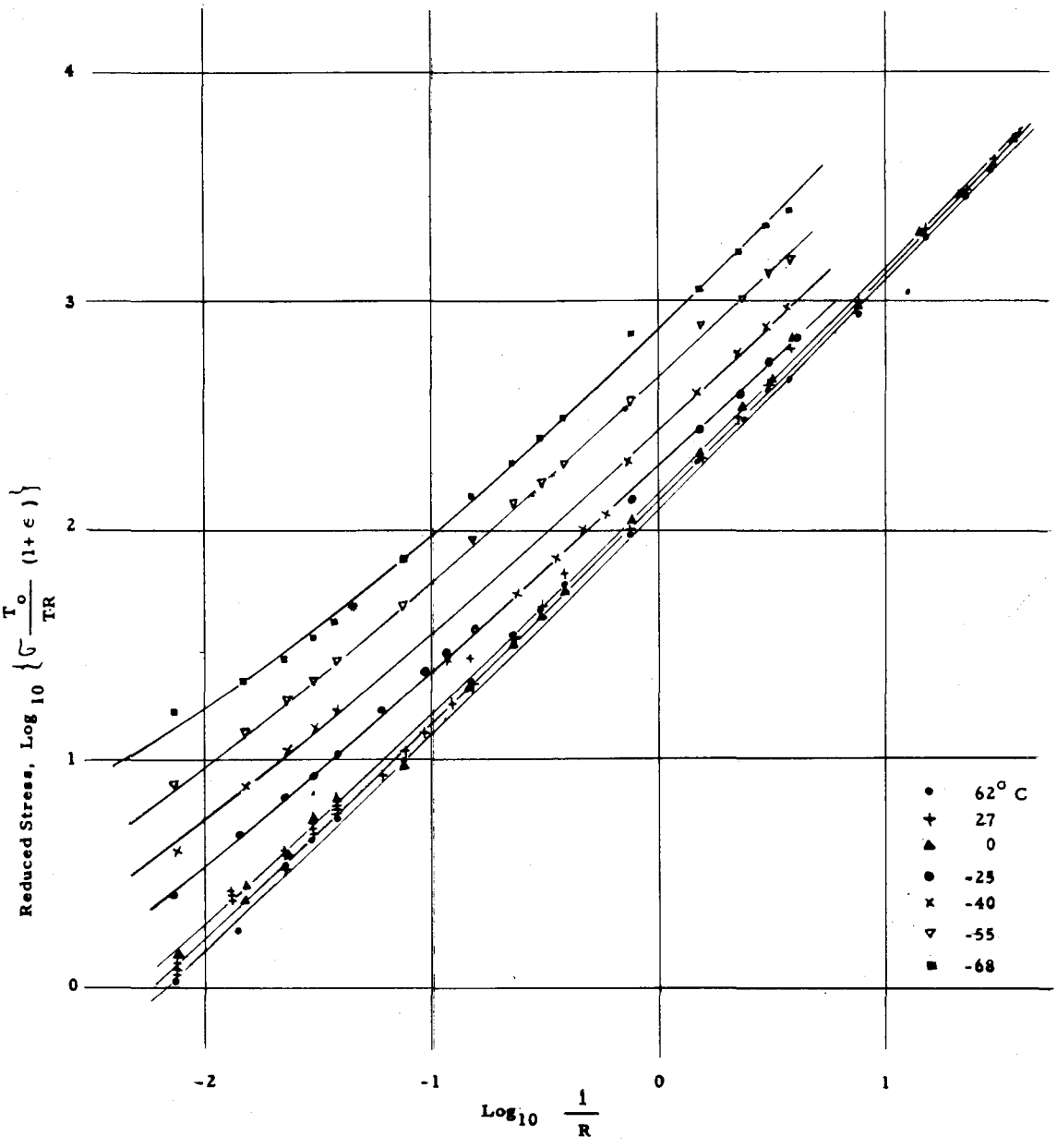

Fig. 7. Stress Strain Curves from Constant Strain Rate Test at Different Temperatures, Unfilled H-C Rubber.

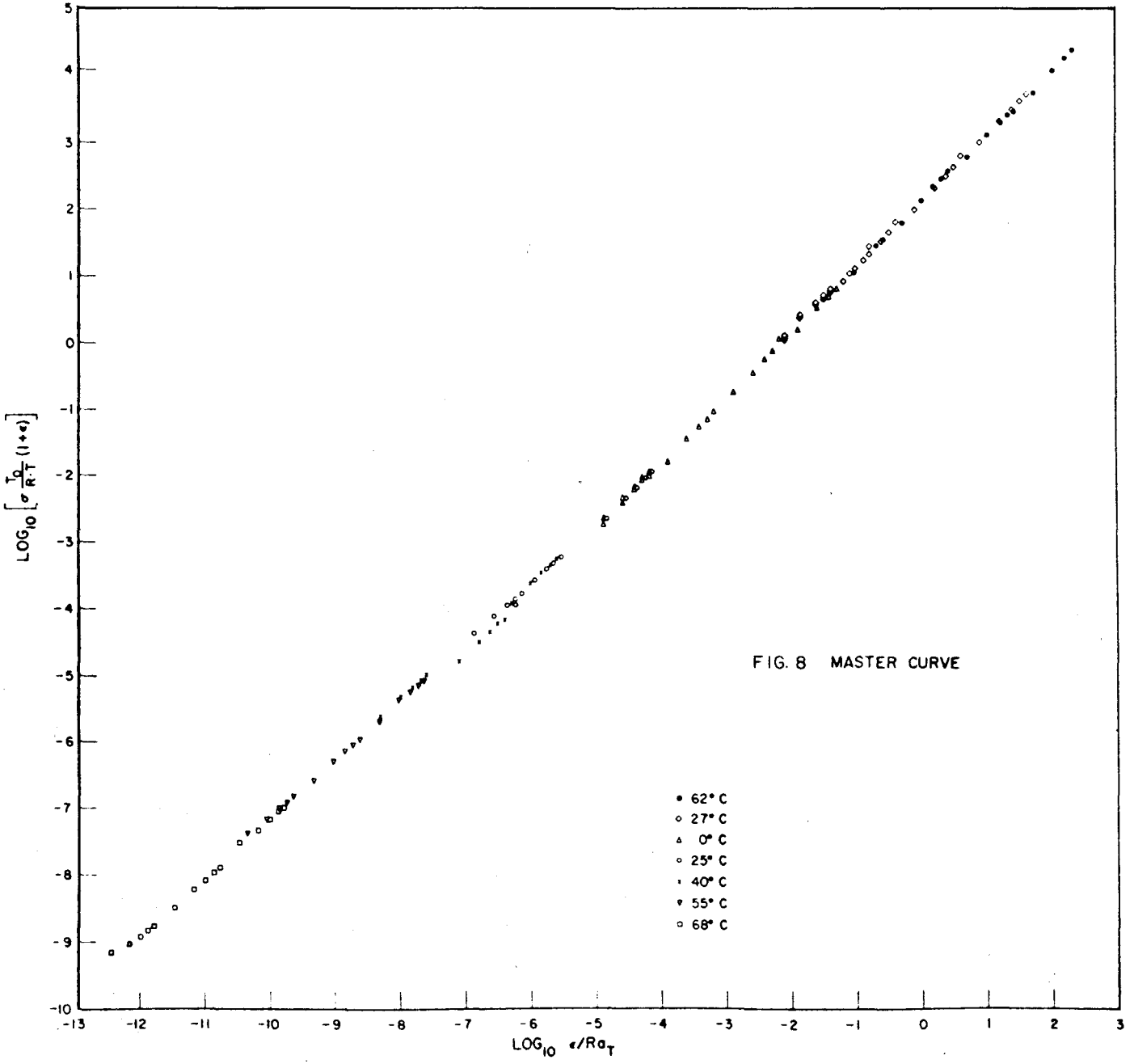

FIG. 8 MASTER CURVE

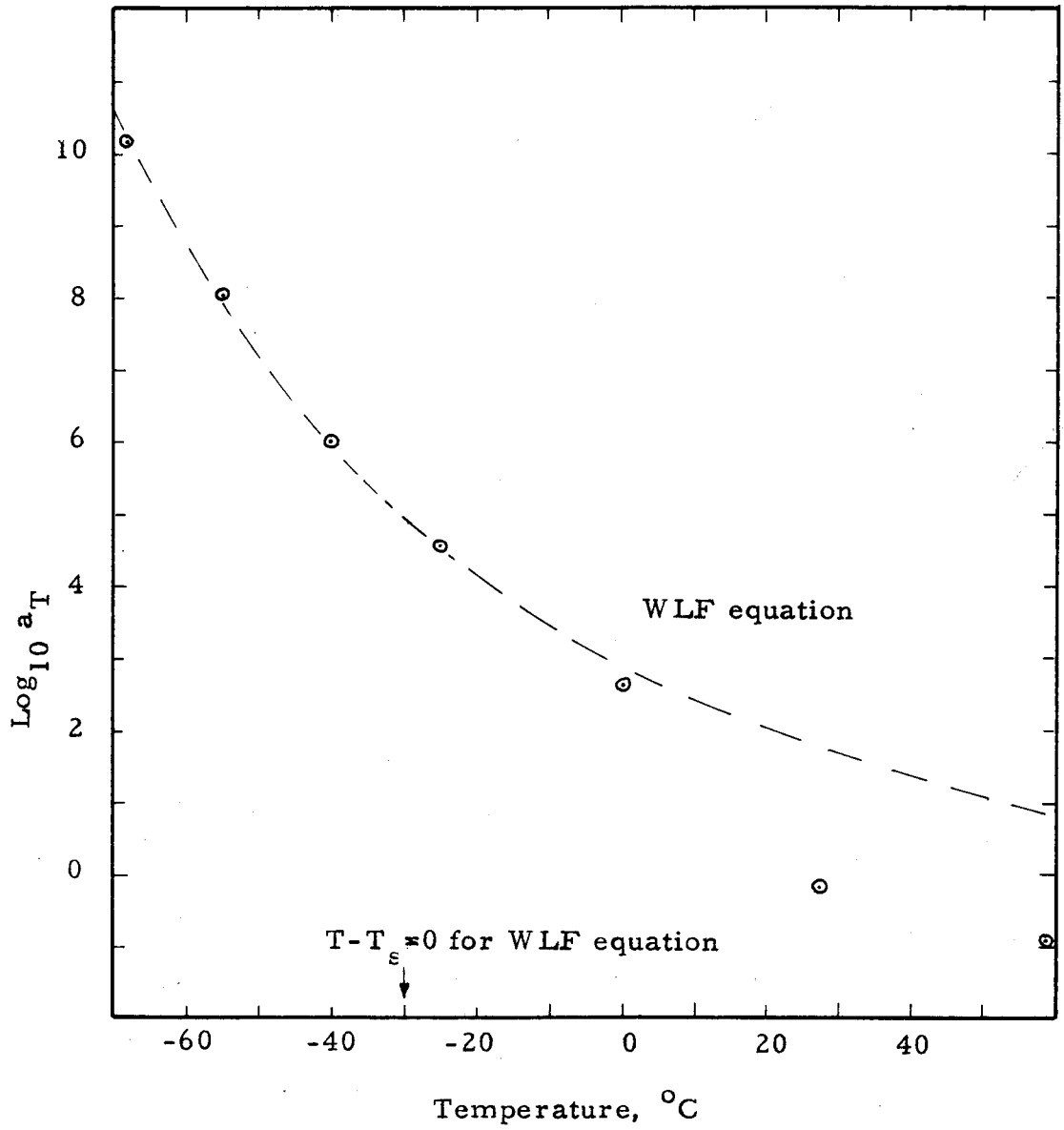

Fig. 9. Shift Factor for Reduction of Stress-Strain Data of Figure 7.

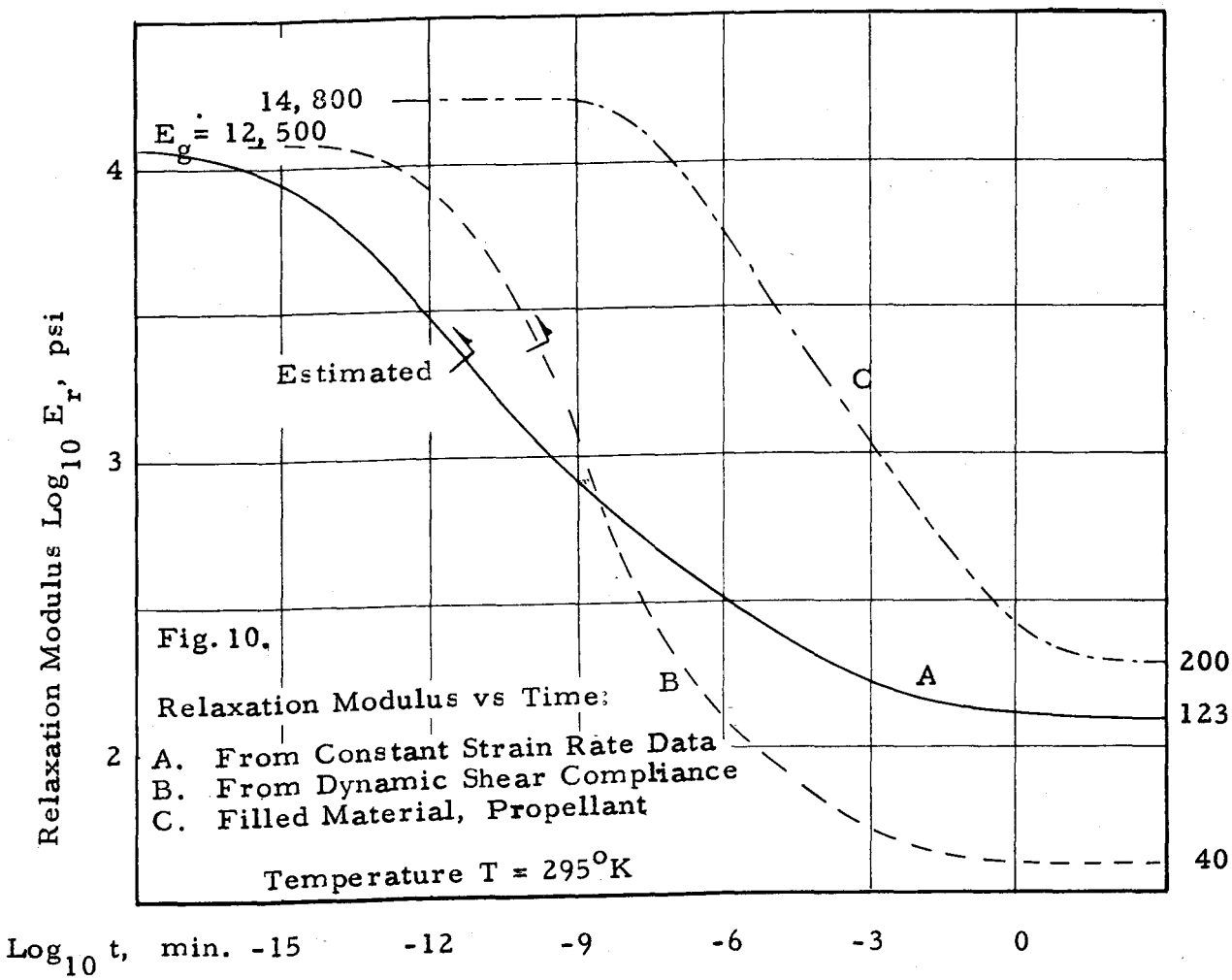
14, 800
E_g = 12, 500
Estimated
C
B
A
200
123
40
Relaxation Modulus $Log_{10} E_r$, psi
4
3
2
Fig. 10.
Relaxation Modulus vs Time:
A. From Constant Strain Rate Data
B. From Dynamic Shear Compliance
C. Filled Material, Propellant
Temperature T = 295°K
Log_{10} t, min. -15 -12 -9 -6 -3 0

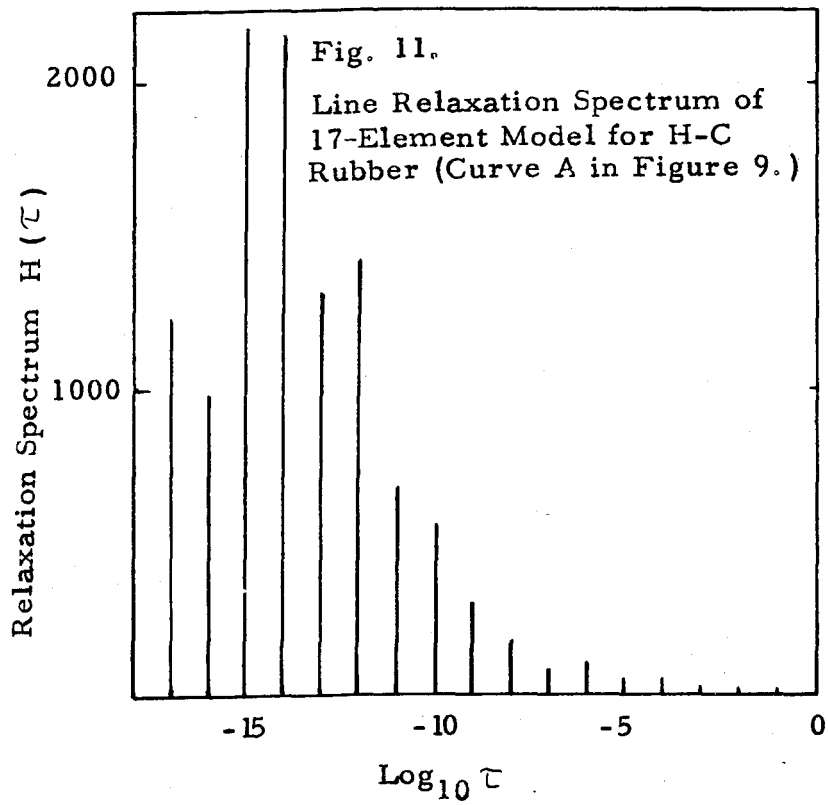
Fig. 11.
Line Relaxation Spectrum of 17-Element Model for H-C Rubber (Curve A in Figure 9.)
2000
1000
Relaxation Spectrum H (τ)
-15
-10
-5
0
$Log_{10} \tau$

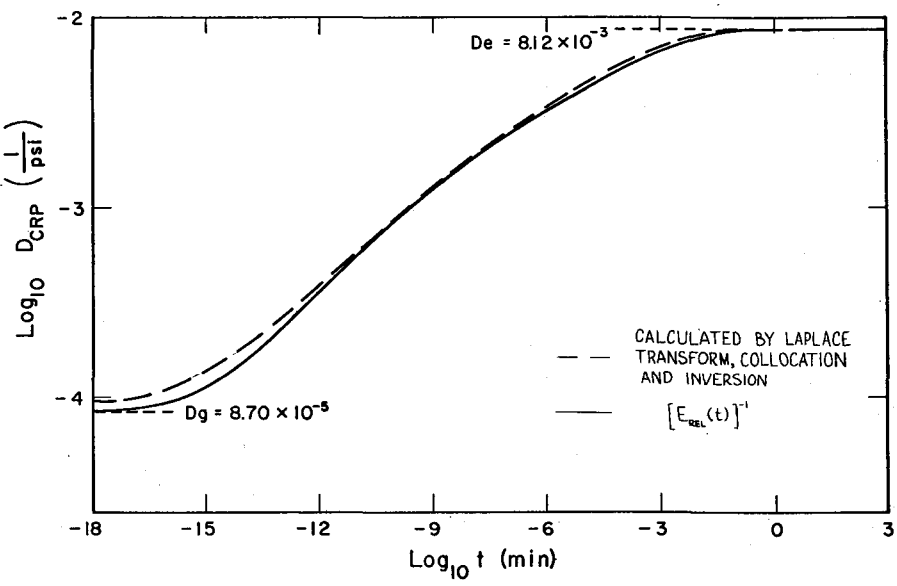

FIGURE 12. CREEP COMPLIANCE.

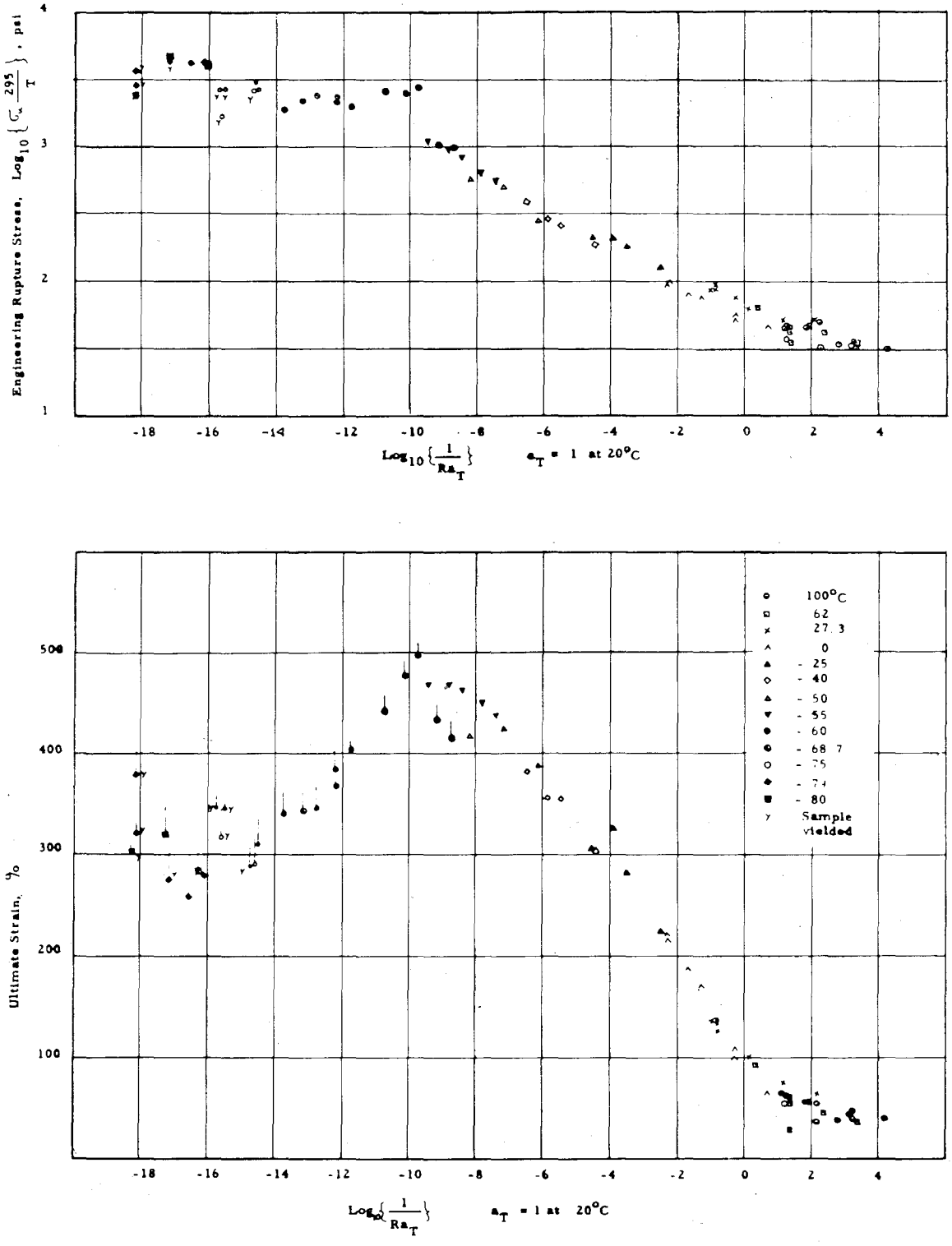

Fig. 13. Ultimate Stress and Strain in a Constant Strain Rate Test; Unfilled H-C Rubber.

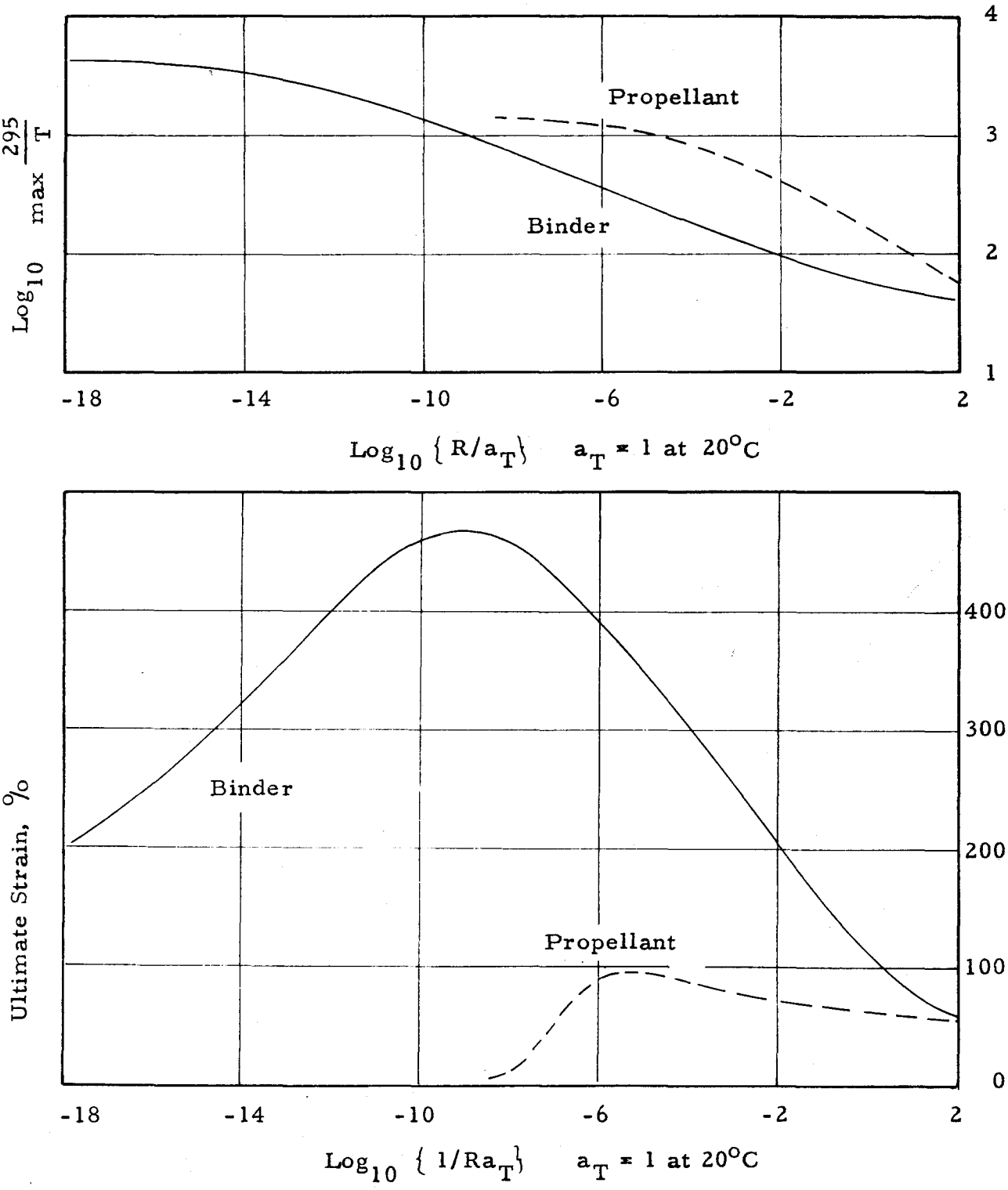

Fig. 14. Ultimate Stress and Strain as a Function of Strain Rate in Uniaxial Tensile Test. For H-C Binder and H-C Propellant (Propellant Data taken from Ref. 1).